4455

Model-Based Reconstruction for Joint Estimation of Multiple Quantitative Maps in the Liver Using Single-Shot IR Multi-Echo Radial FLASH

Vitali Telezki[1,2,3,4], Daniel Mackner[5], Nick Scholand[2,5], Zhengguo Tan[6], Moritz Blumenthal[5], Philip Schaten[5], Xiaoqing Wang[7], and Martin Uecker[1,2,3,5,8]
[1]Department of Interventional and Diagnostic Radiology, University Medical Center Göttingen, Göttingen, Germany, [2]German Centre for Cardiovascular Research (DZHK), partner site Lower Saxony, Göttingen, Germany, [3]Cluster of Excellence Multiscale Bioimaging: from Molecular Machines to Networks of Excitable Cells (MBExC2067), University of Göttingen, Göttingen, Germany, [4]Department of Neurology, University Medical Center Göttingen, Göttingen, Germany, [5]Institute of Biomedical Imaging, Graz University of Technology, Graz, Austria, [6]Michigan Institute for Imaging Technology and Translation (MIITT), Radiology, University of Michigan, Ann Arbor, MI, United States, [7]Department of Radiology, Boston Children's Hospital, Harvard Medical School, Boston, MA, United States, [8]BioTechMed-Graz, Graz, Germany

Synopsis

Keywords: Quantitative Imaging, Quantitative Imaging, Joint Estimation

Motivation: Rapid acquisition and reconstruction of high-quality liver water-specific T_1, R_2^*, B_0 field, and fat-fraction maps to enhance diagnostic feasibility and to improve patient comfort.

Goal(s): Integrating a multi-parameter-sensitive sequence with advanced model-based reconstruction to jointly estimate quantitative maps from 4-second acquisitions.

Approach: Integrate an analytical signal model into a calibration-free, model-based reconstruction framework to jointly estimate water-specific T_1, R_2^*, B_0 field, and fat-fraction maps of the liver from a 4-second single-shot inversion-recovery multi-echo radial FLASH acquisition.

Results: Numerical phantom study and in-vivo liver reconstructions demonstrate high quantitative accuracy for all parameter maps.

Impact: By combining a highly sensitive sequence with model-based reconstructions, this work reduces acquisition times for quantitative water-specific T_1, R_2^*, B_0 field and fat-fraction maps to 4s and makes quantitative multi-parametric MRI more accessible and convenient for diagnostic purposes.

Introduction

Quantitative water-specific $T_1,\ R_2^*$ and fat-fraction (FF) imaging is of great interest in liver imaging[1,2]. However, conventional methods are typically time-intensive, since they require individual data acquisition for each map. Therefore, to enable efficient acquisition, constraints have been developed to facilitate quantitative parameter mapping. In particular, techniques like MR fingerprinting[3,4] or multitasking[5] allow for simultaneous mapping of water-specific $T_1,\ T_2$ and R_2^* by utilizing multi-echo readout schemes. However, instead of performing non-linear fitting of the reconstructed images to the underlying physical model, here we apply a fully non-linear model to reconstruct water-specific $T_1,\ R_2^*$, FF and in addition, B_0 field maps directly from k-space data.[6]

Methods

We combine a single-shot inversion recovery (IR) sequence with a multi-echo radial FLASH readout and incorporate blip gradients between echoes for improved k-space coverage[7] (Fig. 1). To jointly estimate water-specific $T_1,\ R_2^*,\ B_0$, and FF maps directly from the acquired k-space data, we model the underlying physical signal and formulate parameter estimation as a non-linear inverse problem. We apply smoothness promoting regularization on the B_0 and joint wavelet sparsity on the other parameter maps as prior knowledge.

Data Acquisition

The sequence starts with a non-selective inversion pulse, followed by a continuous multi-echo radial FLASH readout (Fig. 1). Radial spokes are rotated along the echo dimension using blip gradients. The trajectory is chosen to cover k-space uniformly. Spokes from all echoes (colors) and several TRs are grouped and distributed in one k-space frame. The angle of the spoke corresponding to the mth echo and lth shot is given by

$$\Theta_{l,m} = \frac{2\pi}{\mathrm{NE}\cdot\mathrm{NS}}\cdot[(l-1)\cdot\mathrm{NE}+m-1]$$

Here, NE denotes the number of echoes and NS the number of repetitions/shots (TRs). To achieve complementary coverage, spokes acquired in consecutive k-space frames are rotated by a small golden-ratio based angle ($\approx 68.75^\circ$).

Model-Based Reconstruction

The acquired signal for nth inversion time TI and mth echo time TE is described by

$$\begin{aligned} S_{\mathrm{TI}_n,\mathrm{TE}_m} &= \Big[W_{\mathrm{ss}} - (W_{\mathrm{ss}}+W_0)\cdot\exp\Big(-R_{1,\mathrm{W}}^*\cdot\mathrm{TI}_n\Big) \\ &\quad + z_m\cdot\Big(F_{\mathrm{ss}}-(F_{\mathrm{ss}}+F_0)\cdot\exp\Big(-R_{1,\mathrm{F}}^*\cdot\mathrm{TI}_n\Big)\Big)\Big] \\ &\quad \cdot\exp\big(i2\pi f_{\mathrm{B}_0}\cdot\mathrm{TE}_m\big)\cdot\exp(-R_2^*\cdot\mathrm{TE}_m) \end{aligned}$$

where W_{ss} (F_{ss}) is the water (fat) specific steady-state signal, W_0 (F_0) the equilibrium-state signal of water (fat) and $R_{1,\mathrm{W}}^*$ ($R_{1,\mathrm{F}}^*$) the effective longitudinal relaxation rate for water (fat). The 6-peak fat spectrum[8] is denoted by z_m, f_{B_0} denotes the field inhomogeneity, and R_2^* is the effective transverse relaxation rate. Applying the signal model, the non-linear forward operator can be written as

$$F: x \mapsto y = \mathcal{PFC}\cdot S_{\mathrm{TI}_n,\mathrm{TE}_m}(x_p)$$

with the radial sampling pattern $\mathcal{P}$, coil sensitivities $\mathcal{C}$ and Fourier transform $\mathcal{F}$. Simultaneous estimation of $x=(x_p,x_c)$ with parameter maps x_p and coil sensitivities x_c is formulated as an optimization problem

$$\hat{x} = \mathrm{argmin}_{x\in D}\sum_{\mathrm{TI}}\sum_{\mathrm{TE}}\|\mathcal{PFC}\cdot S_{\mathrm{TI}_n,\mathrm{TE}_m} - Y_{\mathrm{TI}_n,\mathrm{TE}_m}\|_2^2 + R(x)$$

with the regularization term $R(\cdot)$. Here, we utilize ℓ_1-wavelet regularization on $\Big(W_{\mathrm{ss}}, W_0, R_{1,\mathrm{W}}^*, F_{\mathrm{ss}}, F_0, R_{1,\mathrm{F}}^*, R_2^*\Big)^{\mathrm{T}}$ and Sobolev regularization on f_{B_0} and coil sensitivity maps. The optimization is solved iteratively using IRGNM-FISTA[9-12] implemented and performed in BART[13].

In-Vivo Data

In-vivo liver data (320x320x6 mm^3) was acquired from 3 healthy volunteers on a 3T Siemens Magnetom Vida after written informed consent. To assess repeatability, scan-rescan tests were performed. All abdominal scans were performed with a combined thorax and spine coil with 26 channels during a brief breath-hold.

Results & Discussion

First, we validated the proposed model-based reconstruction on a numerical phantom (BART) (Fig. 2a). The presented numerical phantom covers a wide range of ground-truth values (T_1:[200:3000]ms, R_2^*:[5:100]s^{-1}, FF[0,80]%, B_0:[-50:50]Hz). Comparison of the 11 ROI-averaged values to the ground truth shows overall low mean differences (Fig. 2b). The low standard deviation indicates high quantitative precision of the proposed method over a large range of values.
For in-vivo liver studies, reference maps for R_2^*, FF, and B_0 were estimated using model-based reconstruction of steady-state multi-echo data.[14] Steady-state data was extracted from the last 140 excitations of the same data. T_1 references were estimated using single-shot IR FLASH with single-echo readout[12]. Figure 3 shows reconstructed maps from a healthy volunteer. To assess accuracy, ROI averaged mean values (red dotted box) of reference data and data acquired with the here proposed method were compared to their difference (see Fig. 4). Overall, the results are in good agreement between reference and the proposed method. Additionally, a small (~1%) within-subject coefficient of variation for T_1 values indicates robustness of the proposed method. Furthermore, the proposed method also enhances precision details in some maps.

Conclusions

We combined a non-linear model-based reconstruction with radial IR multi-echo FLASH acquisition enabling joint estimation of accurate water-specific $T_1,\ R_2^*$, FF, and B_0 field maps from a single-shot acquisition of four seconds while maintaining high accuracy. Our developed method can potentially improve patient comfort and add valuable diagnostic information while simultaneously rendering multi-parametric qMRI more feasible for clinical applications.

Acknowledgements

This work was funded by the Deutsche Forschungsgemeinschaft (DFG, German Research Foundation) under grants UE 189/4-1 and TA 1473/2-1 and under Germany's Excellence Strategy - - EXC 2067/1-390729940. Supported by research grant from Else Kröner-Freseniuus Foundation and by the DZHK (German Centre for Cardiovascular Research), funding code: 81Z0300115.

References

1. Xia, T. et al. Association between Liver MRI Proton Density Fat Fraction and Liver Disease Risk. Radiology 309, e231007 (2023).
2. Margaret Cheng, H.-L., Stikov, N., Ghugre, N. R. & Wright, G. A. Practical medical applications of quantitative MR relaxometry. Journal of Magnetic Resonance Imaging 36, 805–824 (2012).

3. Ma, D. et al. Magnetic resonance fingerprinting. Nature 495, 187–192 (2013).
4. Jaubert, O. et al. Multi-parametric liver tissue characterization using MR fingerprinting: Simultaneous T1, T2, T2*, and fat fraction mapping. Magnetic Resonance in Medicine 84, 2625–2635 (2020).
5. Wang, N. et al. Free-breathing multitasking multi-echo MRI for whole-liver water-specific T1, proton density fat fraction, and quantification. Magnetic Resonance in Medicine 87, 120–137 (2022).
6. Wang, X. et al. Model-Based Reconstruction for Joint Estimation of T_1, R_2^* and B_0 Field Maps Using Single-Shot Inversion-Recovery Multi-Echo Radial FLASH. Preprint at https://doi.org/10.48550/arXiv.2402.05366 (2024).
7. Tan, Z., Voit, D., Kollmeier, J. M., Uecker, M. & Frahm, J. Dynamic water/fat separation and inhomogeneity mapping—joint estimation using undersampled triple-echo multi-spoke radial FLASH. Magnetic Resonance in Medicine 82, 1000–1011 (2019).
8. Yu, H. et al. Multiecho water-fat separation and simultaneous R estimation with multifrequency fat spectrum modeling. Magnetic Resonance in Medicine 60, 1122–1134 (2008).
9. Bakushinsky, A. B. & Kokurin, M. Y. Iterative Methods for Approximate Solution of Inverse Problems. (Springer Science & Business Media, 2005).
10. Engl, H. W., Hanke, M. & Neubauer, A. Regularization of Inverse Problems. (Springer Science & Business Media, 1996).
11. Beck, A. & Teboulle, M. A Fast Iterative Shrinkage-Thresholding Algorithm for Linear Inverse Problems. SIAM J. Imaging Sci. 2, 183–202 (2009).
12. Wang, X. et al. Model-based T1 mapping with sparsity constraints using single-shot inversion-recovery radial FLASH. Magnetic Resonance in Medicine 79, 730–740 (2018).
13. Uecker, M. et al. Software toolbox and programming library for compressed sensing and parallel imaging. in ISMRM Workshop on Data Sampling and Image Reconstruction 41 (Sedona, 2013).
14. Tan, Z. et al. Free-Breathing Liver Fat, R_2* and B_0 Field Mapping Using Multi-Echo Radial FLASH and Regularized Model-Based Reconstruction. IEEE Transactions on Medical Imaging 42, 1374–1387 (2023).

Figures

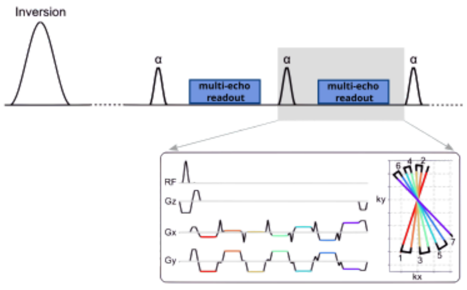

Fig.1: Diagram of a radial single-shot inversion-recovery multi-echo FLASH sequence with corresponding trajectory in k-space. Spokes from several shots (TRs) and all echoes (colors) are distributed equally in one k-space. Each k-space is rotated by a small golden-ratio based angle after each multi-echo readout.

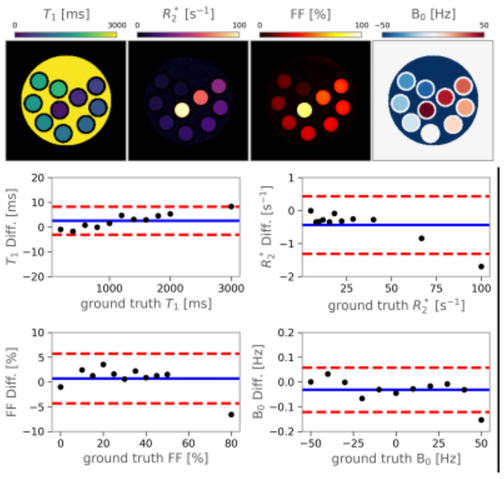

Fig.2: *Top:* Reconstructed T_1, R_2^*, FF, and B_0 field maps from the numerical phantom study simulated with BART[13]. The phantom contains 11 ROIs (10 tubes + background) and covers a wide range of parameter values. *Bottom:* Difference plots comparing the ROI-averaged values to the ground truth values used in the simulation.

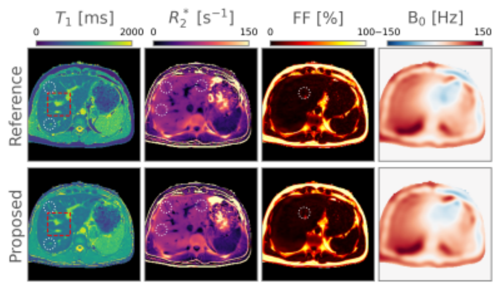

Fig.3: Reconstructed T_1, R_2^*, FF, and B_0 field maps from the in-vivo study on a liver. *Top row:* Reference maps reconstructed from single-shot IR acquisition (T_1) and steady-state single-shot multi-echo acquisitions (R_2^*, FF,B_0). *Bottom row*: Joint reconstructions of the proposed single-shot IR multi-echo acquisition. Red box marks the analyzed ROI, white circles highlight regions with improved details.

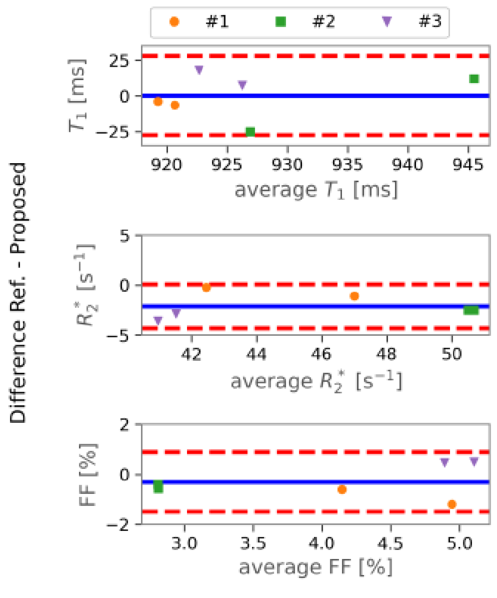

Fig.4: Bland–Altman plots of the ROI analysis comparing results of 3 different healthy volunteers each incorporating a scan-rescan test. The blue solid line indicates the mean and the red dotted lines indicate the $\pm 1.92\sigma$ range around the mean.

Proc. Intl. Soc. Mag. Reson. Med. 33 (2025)
4455